FISEVIER

Contents lists available at ScienceDirect

Chemical Physics Impact

journal homepage: www.sciencedirect.com/journal/chemical-physics-impact



Full Length Article

Design, synthesis of new 4,5-dibenzylidene-9,10-diphenyl-1,2,7,8,9,10 hexahydroacridine-3,6-dione derivatives using extract of *Vitexnegundo*: Cytotoxic activity & molecular docking study

Perumal Gobinath ^a, Ponnusamy Packialakshmi ^a, Govindasamy Thilagavathi ^b, Natarajan Elangovan ^c, Renjith Thomas ^{d,*}, Radhakrishnan Surendrakumar ^{a,*}

- ^a Research Department of Chemistry, Nehru Memorial College (Affiliated Bharathidasan University), Puthanamapatti, Tamilnadu, India
- b PG & Research Department of Physics, Nehru Memorial College (Affiliated Bharathidasan University), Puthanamapatti, Tamilnadu, India
- ^c Centre for Theoretical and Computational Chemistry, St Berchmans College (Autonomous), Mahatma Gandhi University, Changanassery, Kerala, 686101, India
- d Department of Mechanical Engineering, University Centre for Research & Development Chandigarh University, Gharuan, Mohali, Punjab, India

ARTICLE INFO

Keywords: Silver nanoparticles Vitex negundo extract Acridinedione analogues Cytotoxicity Molecular docking

ABSTRACT

Among phytochemical and pharmaceutical investigations, the green production of silver nanoparticles has emerged as the crown jewel of this investigation. The production of acridinedione substances is greatly aided by the high catalytic activity of these nanoparticles. Structures and morphologies were determined by using a wide range of analytical techniques, including nuclear magnetic resonance (1 H & 13 C), Fourier transform infrared spectroscopy, mass spectrometry, elemental investigation, scanning electron microscopy, also transmission electron microscopy. Acridinedione compounds' cytotoxicity was measured using the MTT assay with doxorubicin as the reference drug in a number of cancerous and healthy cell lines, comprising Human embryonic kidney cell (HEK293), liver cell (LO2), and lung cell (MRC5). The cytotoxicity compound 1h was shown to be especially active (HepG2, LC50-0.5 μ M; MCF-7, LC50-0.64 μ M; HeLa, LC50-0.52 μ M). By eliciting IC50 values larger than 100 μ g/M in normal cell lines (HEK-293), (LO2), and (MRC5), the synthesised compounds proved to be safe. In addition, we present the results from an *in-silico* analysis of the Methoxsalen protein (1211). The binding affinity of compound 1h for the 1Z11 protein is greater than that of other compounds (-11.7 kcal/mol), but it is less than that of Doxorubicin (-10.2 kcal/mol). Hence, the chemical 1h may be used to create powerful cancer drugs.

1. Introduction

In the twenty-first century, cancer remains a significant health concern. Cancer is a hereditary illness that involves several different physical phenomenasuch as cell signalling and death, making treatment difficult [1]. Cancer is often identified as a limited sickness that evolves over time, making therapy tough. It's the leading killer in industrialised nations. Cancer symptoms include new tumour growth, irregular bleeding, prolonged coughing, unexplained weight loss, as well as changes in bowel habits [2]. Yet, the mechanism by which malnutrition increases cancer risk remains obscure [3]. Cancer is the leading cause of death in the United States and has the 2nd highest global mortality rate [4–6]. Several researchers (using radiation and chemotherapy) have spent years trying to figure out how to effectively combat cancer [7]. Chemotherapy is the sole choice for treating cancer that has progressed

to other organs, despite the fact that it has serious side effects similar to those of other treatments. Several noncytotoxic drugs inhibit cancer cell proliferation [8]. The synthesis of nanoparticles with bioactive substance is an attractive nanotechnology that is a component of green chemistry. The term "green chemistry" denotes to the evolution of chemical compounds and procedures that considerably minimise the usage of toxic components or solvents without compromising the ability to produce desirable items at an affordable price. In the wake of the effective development of green nanoparticles (NPs), numerous biological techniques were devised for the manufacture of metal NPs, including the use of enzymes [9], microorganisms [10], and plant extracts [11–13]. A profile of bioactive compounds of *Vitex negundo* has been reported, which revealed that the plant contained a high amount of total phenolic compounds and flavonoids, which are considered to be potent natural antioxidants [14–17]. Two important challenges for the

E-mail addresses: renjith@sbcollege.ac.in (R. Thomas), surendrakumar@nmc.ac.in (R. Surendrakumar).

^{*} Corresponding authors.

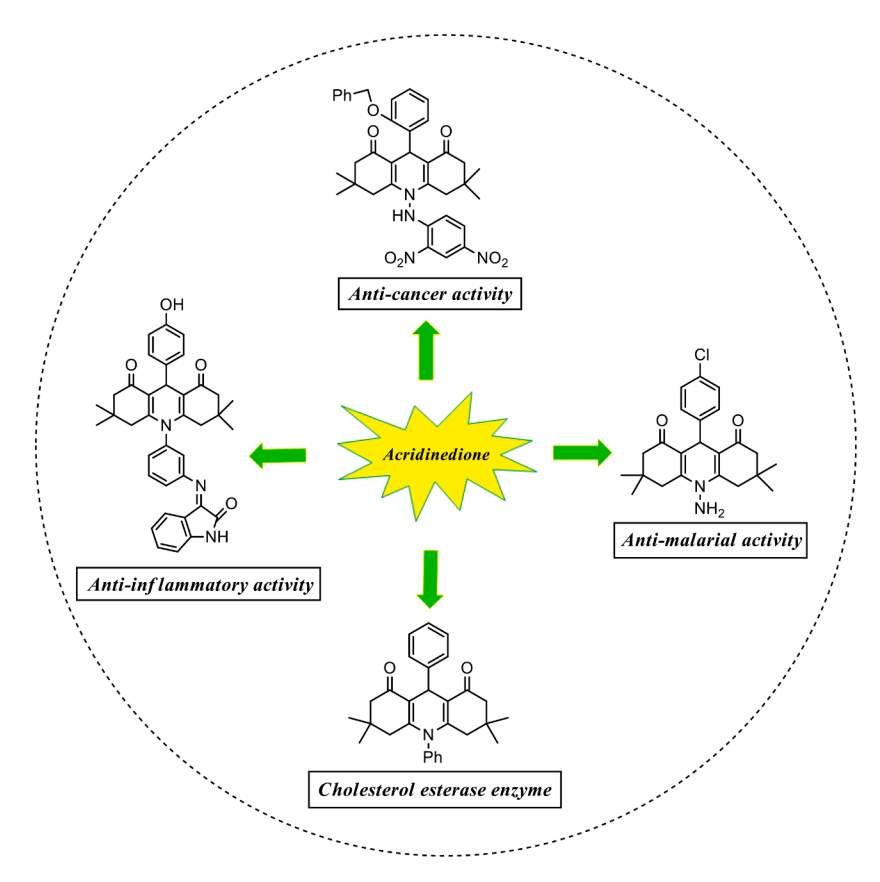


Fig. 1. Biologically active 1,8-acridinedione compounds.

use of acridones as prospective anti-cancer medications are the capacity of acceptor/donor nitrogen to intercalate among base pairs in the double-stranded DNA structure and the efficiency of tricyclic, heterocyclic, and planar arrays to intercalate between base pairs in the double-stranded DNA structure [18,19]. Furthermore, acridone analogues impede the growth of cancer cells through blocking the activity of enzymes that control DNA topology, including topoisomerase, telomerase, and cyclin-dependent kinases [20,21]. Several chemicals with important physiological effects have this basic structure. Antifungal [22], antitumor [23], anticancer [24], and antiglaucoma [25] properties have been shown to be present in acridinedione variants, as shown in Fig. 1. One approach for synthesising acridinedione is the multi component reaction (MCR) of various amines, cyclic diketones, and aldehydes utilising different catalysts [26-27]. DFT has been applied for high accuracy for quantum mechanical electronic structure calculations on the title compound with different solvents. Highest Occupied Molecular Orbital to Lowest Unoccupied Molecular Orbital is investigated in water and DMSO solvent [28–32]. Owing to the difficulty in recycling, recovering, and separating these homogenous catalysts throughout synthesis. To get over these restrictions and enhance the reaction conditions for acridinedione synthesis, a new method using reusable catalyst has been developed. To prepare substituted acridinedione derivatives on ethanol medium with milder process conditions, shortened reaction times, improved substituent variation in the components, and higher yields, we provide a simple and direct approach for the synthesis and characterization of Ag NPs, which are used as a novel and increasingly cost-effective green catalyst. Before evaluating the compounds for cytotoxicity, they were characterised using FT-IR, NMR (¹H-NMR and ¹³C-NMR), mass, elemental analysis, scanning electron microscopy (SEM), and transmission electron microscopy (TEM).

2. Materials and methods

2.1. General methods

1,3-cyclohexanedione, substituted aldehyde, and aniline were all compounds supplied by Merck. The melting points were determined using open capillary tubes that were not calibrated. All of the KBr IR spectra were captured with a Shimadzu 8201 pc (4000-400 cm⁻¹). The ¹H and ¹³C NMR spectra were recorded using a Bruker DRX-300 MHz instrument. The elemental analysis (of C, H, and N) was performed using a model of an elemental analyzer (Varian EL III). The GC-MS data was recorded using a Perkin Elmer GCMS clarus SQ8 (EI). The morphology of silver nanoparticles is verified by scanning electron microscopy and transmission electron microscopy. For SEM analysis, we used a VP-1450 Scanning Electron Microscope from LEO (a German company). For this work, researchers used a transmission electron microscopy (TEM) instrument with the name of LEO 912 AB. Silica gel plates and thin layer chromatography were used to analyse the chemicals for purity (TLC).

2.2. Preparation of Vitex negundo extract

Vitex negundo green leaves were washed and dried in an oven dryer at 40 °C for 48 h. The dried leaves were ground into a powder and stored at 20 °C for further analysis. Overnight at 40 °C, 20 grammes of coarsely chopped leaves were extracted with methanol (ratio 1:10 w/v) in a water bath with shaking. A vacuum pump was used to collect the residue again after it had been filtered using Whatman filter paper No. 1. Using a rotational vacuum evaporator maintained at 40 °C, all of the solvent was removed. After the extract was concentrated, it was stored in dark vials at 4 °C.

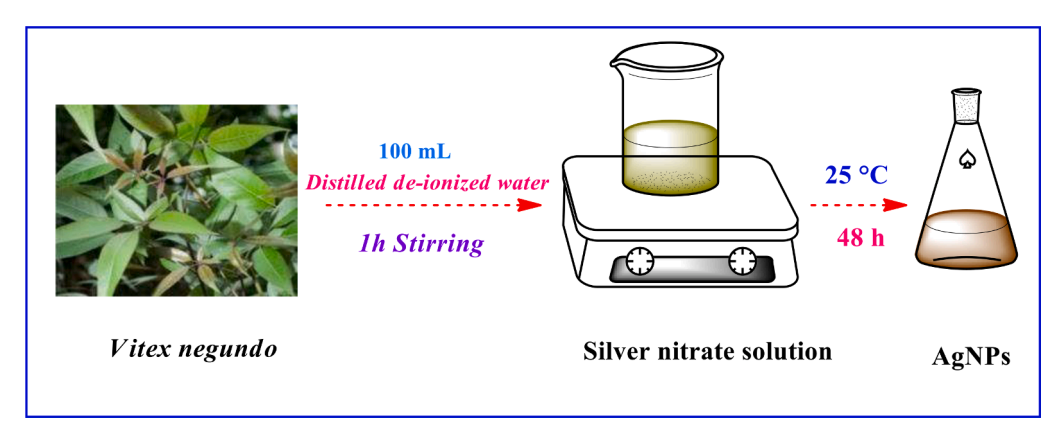


Fig. 2. Synthesis of Ag nanoparticles from Vitex negundo.



Fig. 3. Recyclability of Ag nanoparticle.

Table 1Catalyst recyclability.

Entry	Catalyst use	Yield (%)		
1	1 st	96		
2	$2^{ m nd}$	93		
3	$3^{\rm rd}$	92		
4	4 th	92		
5	5 th	90		
6	6 th	90		
7	7 th	89		
8	8 th	88		
9	9 th	87		
10	$10^{ m th}$	86		

2.3. Synthesis of AgNPs

The crude extract (0.5 g) was vigorously mixed into 100 mL of distilled de-ionized water for 1 hour. Following that, a hundred millilitres (1 \times 10 $^{-1}$ M) of AgNO $_{\!3}$ was weighed and agitated for 48 h at room temperature (25 $^{\circ}$ C). Throughout the incubation period, silver nanoparticles were gradually obtained. The synthesis of Ag-NPs is shown in Fig. 2.

2.4. Recovery of catalyst

Fig. 3 shows the recovery of the catalyst salvaged from at least 10 run times, with a slight loss in catalytic activity. The lessening of activity

could be detected with the regenerated catalyst on salvaging due to the surface area of the catalyst during the reaction, or partial loss of the basic sites/regeneration. The application of the catalyst was inspected by optimizing the reaction conditions. A number of aldehydes were selected for the condensation reaction with the Ag-NPs (1 mole %) catalyst at room temperature in a solvent-free setting, and th0e yield is reported in Table 1.

2.5. General procedure for the synthesis of 4-benzylidene-5-ethylidene-9,10-diphenyl-1,2,7,8,9,10-hexahydroacridine-3,6(4H,5H)-dione (1a)

We compounded substituted 1,3-cyclohexanedione derivative (0.02 mol), benzaldehyde (0.01 mol), and aniline (0.01 mol) as well as AgNPs as a catalyst in ethanol solution to give a yellow precipitate. The product was filtered and dried after being rinsed with ice cold water. TLC was used to validate the product. Ethanol was used to recrystallize the precipitate. Compounds (1b–1j) were synthesized using the same procedure (Scheme 1).

2.6. Cytotoxic activity

The newly synthesized compounds (1a–1j) were screened for their cytotoxic activity according to a procedure described in previous literature [33]. Three cancer cell lines were treated with these compounds at one primary cytotoxic assay dose of $100~\mu M$ for 48 h (MTT anticancer assay). Doxorubicin was used as a standard. The three cell lines used in the present investigation were HepG2 (liver) and Hela (cervical), MCF-7

Table 2 Cytotoxic activity of synthesized compounds (1a-1j)^a.

Cpds		MCF7		HeLa			HepG2		
	GI ₅₀ (μΜ)	TGI (μM)	LC ₅₀ (μΜ)	GI ₅₀ (μΜ)	TGI (μM)	LC ₅₀ (μM)	GI ₅₀ (μM)	TGI (μM)	LC ₅₀ (μΜ)
1a	-	-	>100	-	-	100 ± 0.02	cb53.2 \pm 0.07	68.3 ± 0.12	>100
1b	56.1 ± 0.04	75.1 ± 0.04	>100	61.0 ± 0.06	79.2 ± 0.05	>100	42.2 ± 0.96	13.1 ± 0.03	56.8 ± 0.03
1c	64.9 ± 0.05	33.7 ± 0.08	39.4 ± 0.28	51.3 ± 0.15	77.2 ± 0.08	66.7 ± 0.10	46.3 ± 0.56	55.3 ± 0.06	59.9 ± 0.06
1d	0.89 ± 0.12	09.3 ± 0.05	65.0 ± 0.38	08.9 ± 0.04	16.8 ± 0.07	55.9 ± 0.08	01.0 ± 0.67	0.25 ± 0.26	54.0 ± 0.08
1e	34.4 ± 0.22	49.3 ± 0.02	66.3 ± 0.09	44.2 ± 0.08	62.1 ± 0.04	>100	25.9 ± 1.56	28.2 ± 0.14	44.8 ± 0.01
1f	28.6 ± 0.08	31.8 ± 0.04	42.3 ± 0.11	31.6 ± 0.11	44.7 ± 0.01	67.4 ± 0.07	39.1 ± 1.47	36.8 ± 0.02	57.5 ± 0.26
1g	12.9 ± 0.16	45.3 ± 0.07	10.3 ± 0.03	52.9 ± 0.01	81.3 ± 0.06	45.3 ± 0.03	21.3 ± 1.63	41.0 ± 0.16	72.1 ± 0.16
1h	44.0 ± 0.04	07.4 ± 0.01	0.64 ± 0.15	07.9 ± 0.03	11.9 ± 0.12	0.52 ± 0.06	2.00 ± 0.86	1.00 ± 0.08	0.50 ± 0.08
1i	55.6 ± 0.10	66.0 ± 0.09	59.3 ± 0.09	59.0 ± 0.08	59.3 ± 0.01	65.0 ± 0.01	29.3 ± 1.26	18.3 ± 0.09	>100
1j	66.0 ± 0.09	39.3 ± 0.08	78.6 ± 0.14	3.3 ± 0.02	48.3 ± 0.09	58.3 ± 0.08	50.3 ± 1.74	35.3 ± 0.02	66.8 ± 0.02
Doxorubicin	0.02 ± 0.05	0.21 ± 0.18	0.74 ± 0.02	0.05 ± 0.10	0.41 ± 0.03	0.88 ± 0.12	0.01 ± 0.58	0.13 ± 0.04	0.58 ± 0.01
(standard)									

^a Each compound was tested in triplicate. All error bars represent mean±SD from three independent experiments.

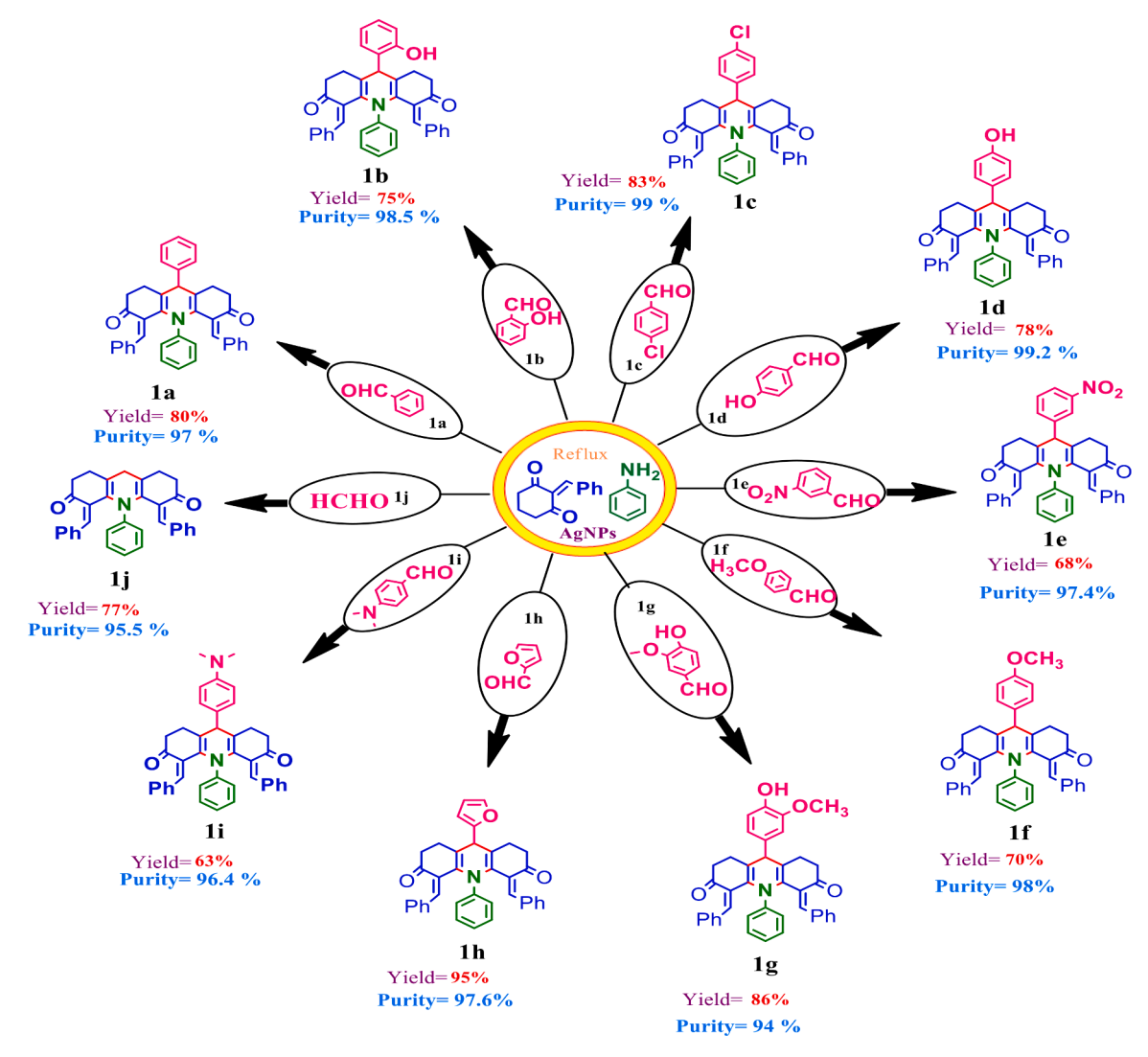


Fig. 4. Optimization of reaction conditions (1a-1j).

(breast). In the current protocol, all cell lines were pre-incubated on a microtiter plate. The results of each test were reported as the growth percentage of treated cells compared to untreated control cells (Table 2). The screening results were expressed in terms of the growth inhibitor concentration (GI $_{50}$), total growth of inhibition (TGI), and lethal concentration (LC $_{50}$). To each well of the 96-well plates, 10,000 cells were

added and incubated in a CO₂ incubator for 24 h at 37° C. Then, the medium was flicked off, and 95 μL of fresh medium and 5 μL of drug were added. The plate was incubated for 48 h at 37° C. The 20 μL medium was removed, 20 μL of MTT was added, and the assay was done. The plate was again incubated in CO₂ incubator for 4–6 h at 37° C. The entire medium was carefully removed, and the formazan crystal solution

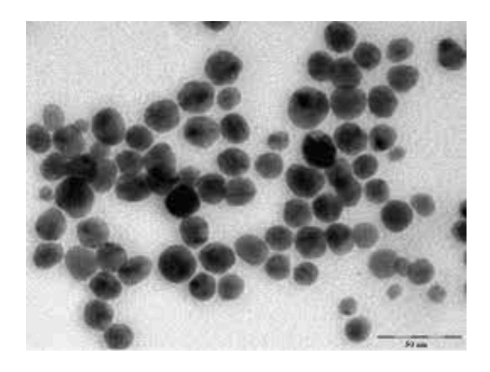


Fig. 5. TEM image of silver nanoparticle.

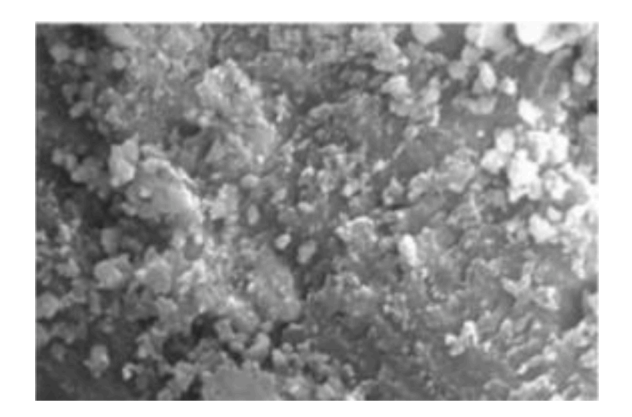


Fig. 6. SEM micrograph of the synthesized AgNPs using *Vitex negundo* leaves extract.

Table 3 In vitro cytotoxicity of synthesised derivatives (1a-1j) on normal cells^a.

Compounds	MRC5 IC ₅₀ (μM)	HEK-293 IC ₅₀ (μM)	LO2 IC ₅₀ (μM)
1a	$\textbf{56.36} \pm 0.08$	$\textbf{69.06} \pm 0.12$	67.48 \pm 0.12
1b	$\textbf{77.21}\pm0.02$	$\textbf{62.12} \pm 0.07$	$\textbf{70.17} \pm 0.18$
1c	$\textbf{76.66} \pm 0.04$	$\textbf{51.14} \pm 0.01$	$\textbf{79.10} \pm 0.07$
1d	$\textbf{58.25} \pm 0.09$	$\textbf{76.14} \pm 0.13$	$\textbf{66.24} \pm 0.04$
1e	$\textbf{70.76} \pm 0.18$	$\textbf{57.09} \pm 0.24$	$\textbf{56.01} \pm 0.10$
1f	$\textbf{59.24} \pm 0.34$	$\textbf{66.17} \pm 0.08$	$\textbf{68.24} \pm 0.24$
1g	$\textbf{66.32} \pm 0.47$	67.01 \pm 0.16	$\textbf{58.22} \pm 0.28$
1h	$\textbf{89.61} \pm 0.28$	$\textbf{88.24} \pm 0.34$	$\textbf{80.54} \pm 0.15$
1i	$\textbf{74.41} \pm 0.11$	$\textbf{75.44} \pm 0.01$	$\textbf{65.70} \pm 0.31$
1j	$\textbf{71.14} \pm 0.13$	$\textbf{52.71} \pm 0.09$	$\textbf{70.12} \pm 0.29$

 $^{^{\}rm a}$ Each compound was tested in triplicate. All error bars represent mean $\pm {\rm SD}$ from three independent experiments.

was made up with DMSO solvent. The molecular stain absorbance was read at 570 nm in a plate reader (Bio-Rad Laboratories Inc., CA, and USA). Cell viability was calculated as (Absorbance 570 nm of Test/Absorbance 570 nm of Control) X 100.

2.7. Molecular docking

Compounds 1a-1j, Doxorubicin, and the Human microsomal cytochrome P450 2A6 protein in association with Methoxsalen (PDB ID: 1Z11) were investigated for their binding mechanism and interactions via Autodock vina 1.1.2. [34–36]. The inhibitor is effectively fills the active site cavity without sustainability perturbing the chemical structure. Compounds 1a-1j and Doxorubicin were developed using Chem3D Pro 12.0 and Chem Draw Ultra 12.0. AutoDock Tools 1.5.6 was used to generate the input files used by AutodockVina. The grid coordinates for

the protein of interest are as follows: centre x,y,z: 56.316, 77.155, 60.326; size x,y,z: 24, 20, 20; and spacing 1.0. Exhaustiveness is seen to be represented by the number 8. The default settings for the other Vina docking parameters are not specified. Discovery Studio 2019 was used to visually evaluate the data, with the chemical with the lowest binding affinity value being awarded the highest score.

3. Results and discussion

3.1. Chemistry

The use of silver nanoparticles as a catalyst is shown in Scheme 2 as a potential technique for the manufacture of acridinedione derivative products. It is hypothesised that the silver nano particle induces the polarisation of carbonyl groups, aldehyde, and 1,3-cyclohexanedione. We also think silver nanoparticles set the stage for the synthesis of 1,3-cyclohexanedione analogues and facilitate the creation of the proper imine through a condensation reaction with aniline. Acquired imine undergoes tautomerization to generate enamine. Thus, silver nanoparticles play a role in the formation of two reactive intermediates, I and II, that react via Michael addition to form an adduct and then undergo tautomerization. A water molecule is lost during the tautomerization of the Michael adduct, resulting in a simple intramolecular ring closure and the desired product, 1a-1j. Fig. 4 shows the optimization of reaction conditions (1a-1j).

Mechanism

Synthesis of 4,5-dibenzylidene-9,10-diphenyl-1,2,7,8,9,10-hexahydroacridine-3,6-dione 1a) IR (KBr) (cm $^{-1}$): 3234 (Ar-H), 2850 (-CH $_{2}$), 1710 (C=O), 1110(C-N); 1 H NMR (300 MHz, DMSO-d $_{6}$): 7.64-6.25 (m, 5H, Phenyl), 7.40-7.33 (m, 10H,), 7.30-7.23 (m, 5H, Ph), 6.20 (s, 2H, =CH-Phenyl), 4.43 (s, 1H, CH-Phenyl), 2.98-2.07 (m, 8H, Cyclohexanedione); 13 C NMR (300 MHz, DMSO-d $_{6}$): 194.41, 142.22, 141.23, 140.24, 137.75, 134.56, 132.07, 129.58, 128.69, 127.70, 122.81, 122.41,109.72, 40.33, 35.04, 20.35; EI-MS: 546 (M+, 20%); Elemental analysis (C $_{39}$ H $_{31}$ NO $_{2}$): Calculated: C, 83.84; H, 5.73; N, 2.57%; Found: C, 83.82; H, 5.71; N, 2.55 %.

Synthesis of 4,5-dibenzylidene-9-(2-hydroxyphenyl)-10-phenyl-1,2,7,8,9,10-hexahydro acridine-3,6-dione 1b) IR (KBr) (cm $^{-1}$): 3400 (OH), 3095 (Ar-H), 2855 (-CH $_{\rm 2}$), 1723 (C=O), 1113 (C-N); $^{\rm 1}$ H NMR (300 MHz, DMSO-d $_{\rm 6}$): 7.64-6.25 (m, 5H, Phenyl), 7.40-7.33 (m, 10H, Phenyl- Cyclohexanedione), 7.09-6.83 (m, 4H, Ph-OH), 6.16 (s, 2H, =CH-Phenyl), 5.35 (s, 1H, OH), 4.43 (s, 1H, CH-Phenyl), 2.98-2.07 (m, 8H, Cyclohexanedione); $^{\rm 13}$ C NMR (300 MHz, DMSO-d $_{\rm 6}$): 194.45, 156.16, 141.27, 140.28, 137.79, 134.50, 132.01, 130.42, 129.53, 128.54, 127.95, 127.16, 122.87, 122.68, 122.49, 115.80, 109.71, 35.02, 34.13, 20.34; EI-MS: 591 (M+, 20%); Elemental analysis (C $_{\rm 39}$ H $_{\rm 30}$ N2O4): Calculated: C, 79.30; H, 5.12; N, 4.74 %; Found: C, 79.28; H, 5.10; N, 4.72 %.

Synthesis of 4,5-dibenzylidene-9-(4-chlorophenyl)-10-phenyl-1,2,7,8,9,10-hexahydro acridine-3,6-dione 1c) IR (KBr) (cm $^{-1}$): 3095 (Ar-H), 2860 (-CH $_{\rm 2}$), 1745 (C=O), 1191 (C-N), 748 (C-Cl); $^{\rm 1}$ H NMR (300 MHz, DMSO-d₆): 7.64-6.25 (m, 5H, Phenyl), 7.40-7.33 (m, 10H, Phenyl Cyclohexanedione), 7.37-7.17 (m, 4H, Ph-Cl), 6.21 (s, 2H, =CH-Phenyl), 4.43 (s, 1H, CH-Phenyl),2.98-2.07 (m, 8H, Cyclohexanedione); $^{\rm 13}$ C NMR (300 MHz, DMSO-d₆): 194.42,141.23, 140.34, 140.25, 137.76, 134.57, 132.08, 131.39, 130.40, 129.51, 128.72, 128.53, 127.94, 122.85, 122.46, 109.77, 40.38, 35.09, 20.30; EI-MS: 561 (M+, 20%); Elemental analysis (C₃₉H₃₁NO₃): Calculated: C, 83.40; H, 5.56; N, 2.49 %; Found: C, 83.38; H, 5.54; N, 2.47 %.

Synthesis of 4,5-dibenzylidene-9-(4-hydroxyphenyl)-10-phenyl-1,2,7,8,9,10-hexahydro acridine-3,6-dione 1d) IR (KBr) (cm $^{-1}$): 3400 (OH), 3029 (Ar-H), 2865 (-CH $_{2}$), 1701 (C=O), 1256 (C-N); 1 H NMR (300 MHz, DMSO-d $_{6}$): 7.64-6.25 (m, 5H, Phenyl), 7.40-7.33 (m, 10H, Phenyl- Cyclohexanedione), 7.06-6.63 (m, 4H, Ph-OH), 6.19 (s, 2H, =CH-Phenyl), 5.35 (s, 1H, OH), 4.43 (s, 1H, CH-Ph), 2.98-2.07 (m, 8H, Cyclohexanedione); 13 C NMR (300 MHz, DMSO-d $_{6}$): 194.43, 155.54,

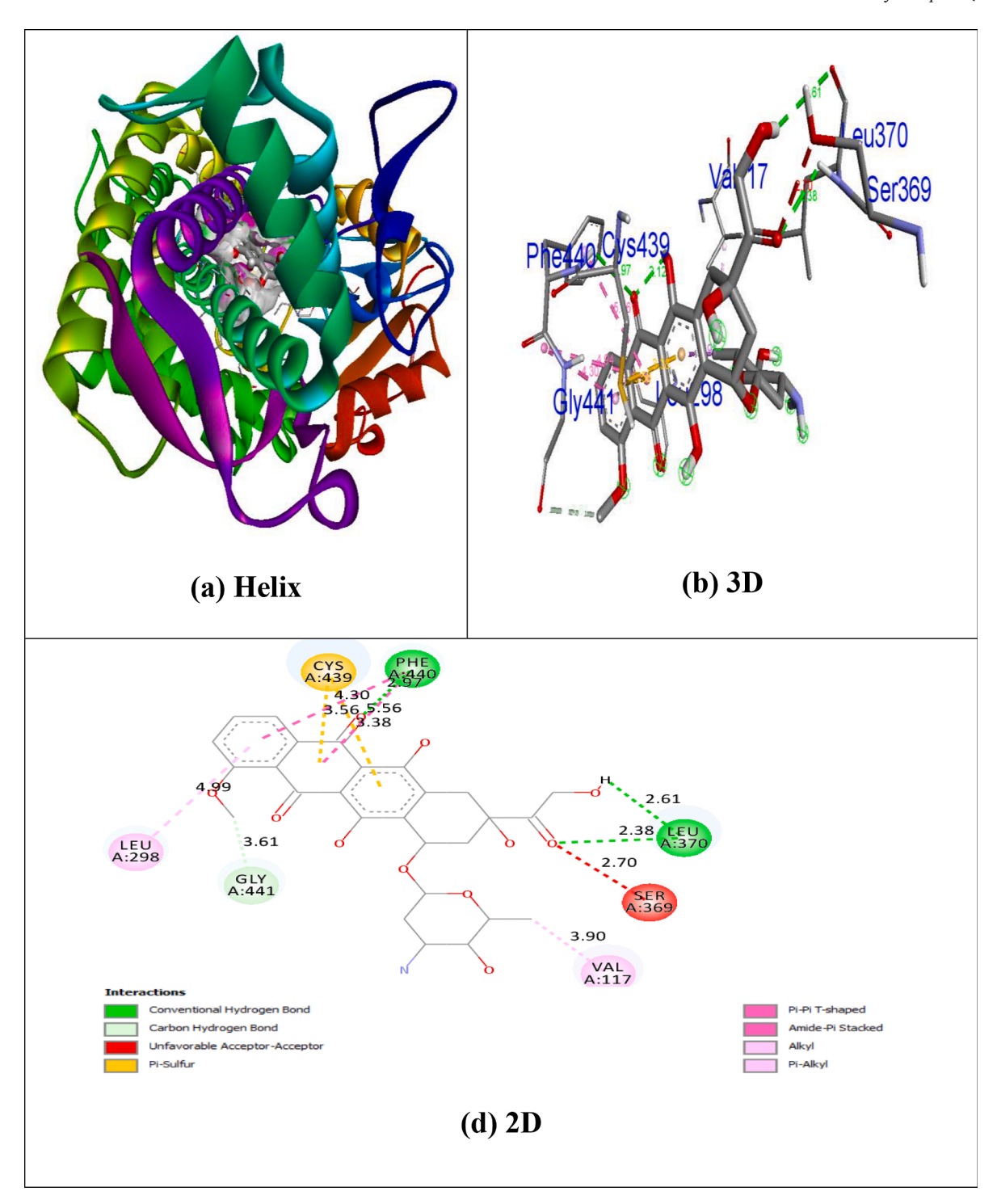


Fig. 7. Interaction kinds of compound 1h in the binding pocket of 1Z11 receptor.

141.25, 140.26, 137.77, 134.88, 134.59, 132.00, 130.41, 129.52, 128.53, 127.94, 122.85, 122.46, 115.87, 109.78, 40.39, 35.00, 20.31; EI-MS: 580 (M+, 20%); Elemental analysis ($C_{39}H_{30}ClNO_2$): Calculated: C, 80.75; H, 5.21; N, 2.41 %; Found: C, 80.73; H, 5.19; N, 2.39 %.

Synthesis of 4,5-dibenzylidene-9-(3-nitrophenyl)-10-phenyl-1,2,7,8,9,10-hexahydroacri dine-3,6-dione 1e) IR (KBr) (cm $^{-1}$): 3027 (Ar-H), 2872 (-CH $_{2}$), 1717 (C=O), 1673 (NO $_{2}$), 1349 (C-N); 1 H NMR (300 MHz, DMSO-d $_{6}$): 8.12-7.62 (m, 4H, Ph-NO $_{2}$), 7.64-6.25 (m, 5H, Phenyl), 7.40-7.33 (m, 10H, Phenyl- Cyclohexanedione), 6.18 (s, 2H, =CH-Phenyl), 5.35 (s, 1H, OH), 4.43 (s, 1H, CH-Phenyl), 2.98-2.07 (m, 8H, Cyclohexanedione); 13 C NMR (300 MHz, DMSO-d $_{6}$): 194.44,

145.25, 143.16,141.27, 140.28, 137.79, 134.50, 133.81, 132.02, 129.53, 128.54, 127.95, 122.86, 122.47, 121.88, 120.99, 109.701, 40.3, 35.02, 20.33; EI-MS: 562 (M+, 20%); Elemental analysis ($C_{39}H_{31}NO_{3}$): Calculated: C, 83.40; H, 5.56; N, 2.49 %; Found: C, 83.38; H, 5.54; N, 2.47 %.

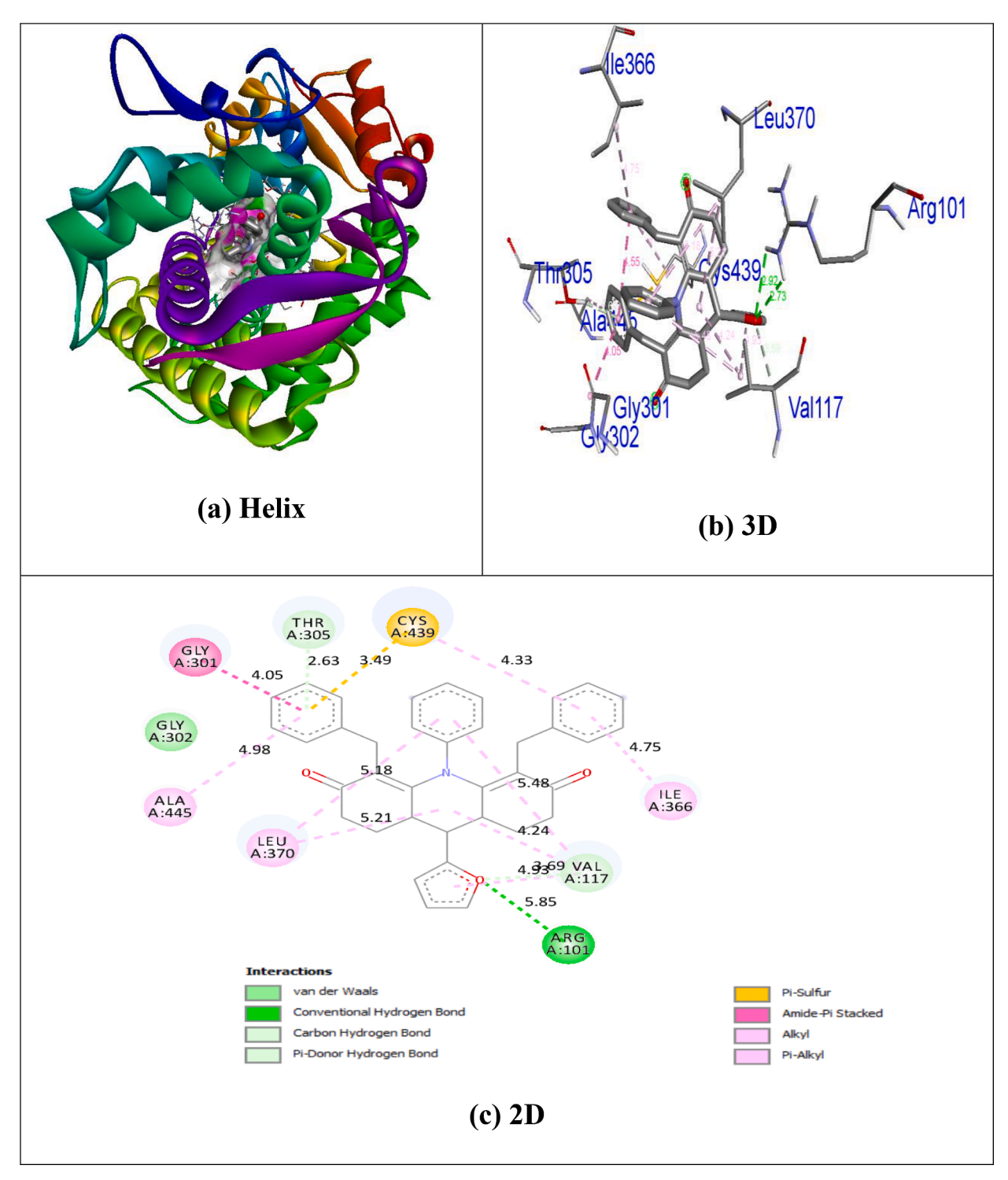
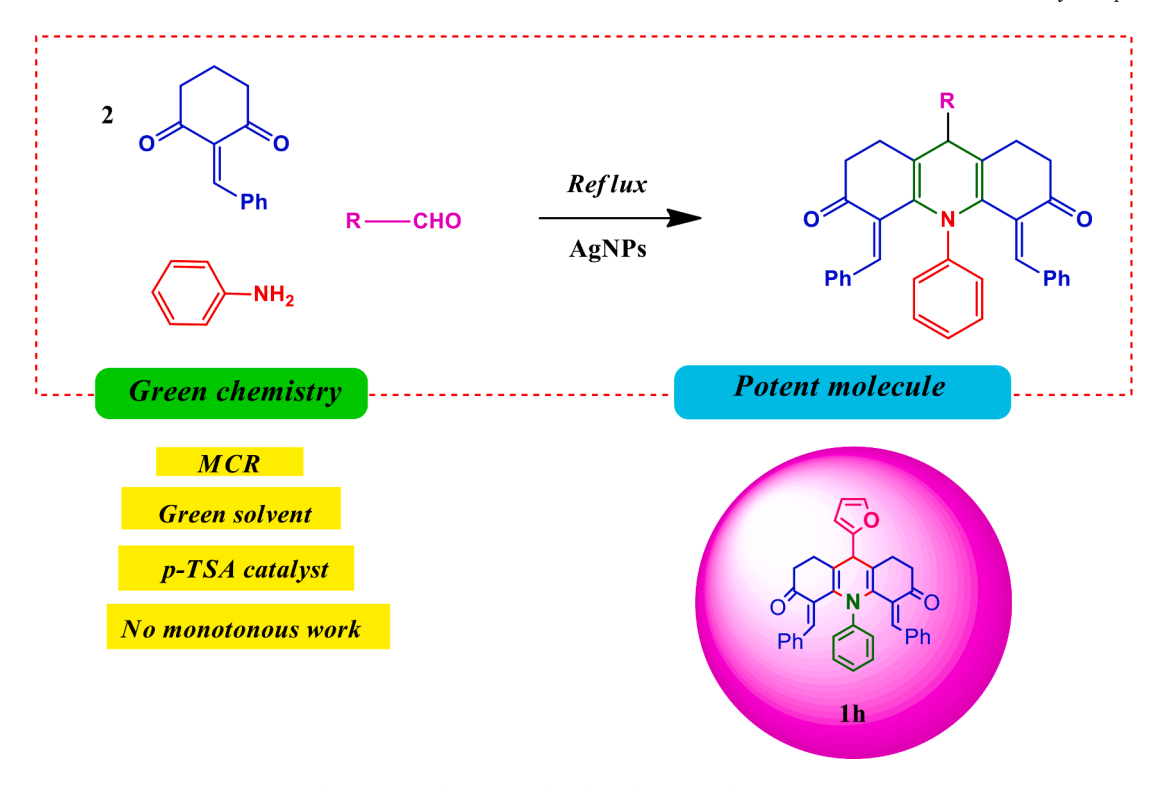


Fig. 8. Interaction kinds of compound Doxorubicin in the binding pocket of 1Z11 receptor.

(m, 8H, Cyclohexanedione); 13 C NMR (300 MHz, DMSO-d₆):194.47, 157.68, 141.29, 140.20, 137.71, 134.52, 132.03, 130.04, 129.55, 128.56, 127.97, 122.88, 122.49, 114.20, 109.71, 55.82, 40.33, 35.04, 20.35; EI-MS: 592 (M+, 20%); Elemental analysis (C₄₀H₃₃NO₄): Calculated: C, 81.20; H, 5.62; N, 2.37 %; Found: C, 81.18; H, 5.60; N, 2.35 %.

van), 6.17 (s, 2H, =CH-Phenyl), 5.35 (s, 1H, OH), 4.43 (s, 1H, CH-Phenyl), 3.83 (s, 3H, -OCH₃), 2.98-2.07 (m, 8H, Cyclohexanedione); 13 C NMR (300 MHz, DMSO-d₆): 194.46, 147.47, 145.78, 141.29, 140.20, 137.71, 135.82, 134.53, 132.04, 129.55, 128.56, 127.97, 122.88, 122.79, 122.40, 115.51, 114.22, 109.73, 56.14, 40.65, 35.06, 20.37; EI-MS: 576 (M+, 20%); Elemental analysis (C₄₀H₃₃NO₃): Calculated: C, 83.45; H, 5.78; N, 2.43 %; Found: C, 83.43; H, 5.76; N, 2.41 %.

 $\label{eq:Synthesis} \begin{array}{lll} \text{Synthesis} & \text{of} & \text{4,5-dibenzylidene-9-(4-(furan-2-yl)phenyl)-10-} \\ \text{phenyl-1,2,7,8,9,10-hexa} & \text{hydroacridine-3,6-dione} & \text{1h}) & \text{IR} & \text{(KBr)} \\ \text{(cm}^{-1}): 3029 & \text{(Ar-H)}, 2925 & \text{(-CH}_2), 1787 & \text{(C=O)}, 1300 & \text{(C-O)}, 1110 & \text{(C-O)} \\ \text{(Com-1)}: 3029 & \text{(Ar-H)}, 2925 & \text{(-CH}_2), 1787 & \text{(C=O)}, 1300 & \text{(C-O)}, 1110 & \text{(C-O)} \\ \text{(Com-1)}: 3029 & \text{(Ar-H)}, 2925 & \text{(-CH}_2), 1787 & \text{(C=O)}, 1300 & \text{(C-O)}, 1110 & \text{(C-O)} \\ \text{(Com-1)}: 3029 & \text{(Ar-H)}, 2925 & \text{(-CH}_2), 1787 & \text{(C=O)}, 1300 & \text{(C-O)}, 1110 & \text{(C-O)} \\ \text{(Com-1)}: 3029 & \text{(Ar-H)}, 2925 & \text{(-CH}_2), 1787 & \text{(C=O)}, 1300 & \text{(C-O)}, 1110 & \text{(C-O)} \\ \text{(Com-1)}: 3029 & \text{(Ar-H)}, 2925 & \text{(-CH}_2), 1787 & \text{(C=O)}, 1300 & \text{(C-O)}, 1110 & \text{(C-O)} \\ \text{(Com-1)}: 3029 & \text{(Ar-H)}, 2925 & \text{(-CH}_2), 1787 & \text{(C=O)}, 1300 & \text{(C-O)}, 1110 & \text{(C-O)}, 1110 & \text{(C-O)} \\ \text{(Com-1)}: 3029 & \text{(Ar-H)}, 2925 & \text{(-CH}_2), 1787 & \text{(C=O)}, 1300 & \text{(C-O)}, 1110 & \text{(C-O)}, 1110 & \text{(C-O)} \\ \text{(Com-1)}: 3029 & \text{(Ar-H)}, 2925 & \text{(-CH}_2), 1787 & \text{(C=O)}, 1300 & \text{(C-O)}, 1110 & \text{(C-O)} \\ \text{(Com-1)}: 3029 & \text{(C-O)}; 3029 & \text{(C-$



Scheme 1. Synthesis of acridinedione derivatives by using AgNPs.

N); ¹H NMR (300 MHz, DMSO-d₆): 7.64-6.25 (m, 5H, Ph), 7.58-6.11 (m, 3H, Phenyl-furfural), 7.40-7.33 (m, 10H, Phenyl- Cyclohexanedione), 6.14 (s, 2H, =CH-Phenyl), 4.43 (s, 1H, CH-Phenyl), 2.98-2.07 (m, 8H, Cyclohexanedione); ¹³C NMR (300 MHz, DMSO-d₆): 194.49, 152.50, 142.11, 141.22, 140.23, 137.74, 132.05, 129.56, 128.57, 127.98, 122.89, 122.40, 110.61, 106.72, 109.73, 41.54, 35.05, 20.36; EI-MS: 589 (M+, 20%); Elemental analysis ($C_{41}H_{36}N_2O_2$): Calculated: C, 83.64; H, 6.16; N, 4.76 %; Found: C, 83.62; H, 6.14; N, 4.74 %.

Synthesis of 4,5-dibenzylidene-9-(4-(dimethylamino)phenyl)-10-phenyl-1,2,7,8,9,10-hexa hydroacridine-3,6-dione 1i)IR (KBr) (cm⁻¹): 3020 (Ar-H), 2967 (-CH₂), 1780 (C=O), 1125 (C-N);¹H NMR (300 MHz, DMSO-d₆): 7.64-6.25 (m, 5H, Phenyl), 7.40-7.33 (m, 10H, Phenyl- Cyclohexanedione), 6.95-6.64 (m, 4H, Phenyl), 6.23 (s, 2H, =CH-Phenyl), 4.43 (s, 1H, CH-Phenyl), 3.83 (s, 3H, OCH₃), 3.06 (s, 6H, -(CH₃₎₂) 2.98-2.07 (m, 8H, Cyclohexanedione); ¹³C NMR (300 MHz, DMSO-d₆): 194.48, 148.19, 141.20, 140.21, 137.72, 132.03, 131.74, 129.55, 128.56, 128.17, 127.98, 122.89, 122.40, 112.01, 109.72, 41.33, 35.04, 20.35; EI-MS: 536 (M+, 20%); Elemental analysis (C₃₇H₂₉NO₃): Calculated: C, 82.97; H, 5.46; N, 2.61 %; Found: C, 82.95; H, 5.44; N, 2.59 %

Synthesis of 4,5-dibenzylidene-10-phenyl-1,2,7,8,9,10-hexahydroacridine-3,6-dione 1j) IR (KBr) (cm $^{-1}$): 3025 (Ar-H), 2955 (-CH₂), 1745 (C=O), 1125 (C-N); 1 H NMR (300 MHz, DMSO-d₆): 7.64-6.25 (m, 5H, Phenyl), 7.40-7.33 (m, 10H, Phenyl- Cyclohexanedione), 6.13 (s, 2H, =CH-Phenyl), 4.43 (s, 1H, CH-Phenyl), 2.98-2.07 (m, 8H, Cyclohexanedione), 3.15 (s, 1H, HCHO); 13 C NMR (300 MHz, DMSO-d₆): 194.40, 141.21, 140.22, 137.73, 132.04, 129.55, 128.56, 127.97, 122.88, 122.49, 109.70, 36.21, 35.02, 20.33; EI-MS: 470 (M+, 20%); Elemental analysis (C₃₃H₂₇NO₂): Calculated: C, 84.41; H, 5.80; N, 2.98 %; Found: C, 84.39; H, 5.78; N, 2.96 %.

3.2. Transmission electron microscopy (TEM)

TEM was used to examine AgNPs for information on their size and shape. TEM image is providing higher resolution and also measure the nanoparticle size. Greenly synthesised AgNPs are spherical and, on average, 20 nm in size, as seen in Fig. 5.

3.3. Scanning electron microscopy (SEM)

The SEM study showed that the AgNPs were tiny, well-defined, and spherical in shape. The huge number of charged surfaces of Vitex negundo makes it a good candidate for chelating metal ions in their aqueous precursor solution. The SEM image shows 13m rang for aggregates of molecules. SEM picture of AgNPs shown in Fig. 6.

3.4. Cytotoxic activity

Compounds 1a-1j are assessed for their cytotoxic potential using a procedure previously published by the US National Cancer Institute [37]. Growth inhibition at 50% (GI₅₀), tumour growth inhibition (TGI), and median lethal concentration (LC₅₀) were determined. After 1 hour, there was considerable action towards (HepG2, LC₅₀-0.52 µM, MCF-7, LC_{50} -0.64 μM , and HeLa, LC_{50} -0.52 μM) with these compounds. Doxorubicin was employed since it is a gold standard medication. Human embryonic kidney (HEK-293), lung (MRC-5), and liver cells were used in the MTT experiment to determine cytotoxicity (LO2). In vitro test findings revealed that these drugs had little to no influence on normal kidney cell development since their IC₅₀ values were all larger than 100. Hence, these compounds have shown that they are not toxic to healthy cells, and compound 1h may serve as a starting point for the creation of even more effective agents against the cancer cell lines HepG2 (liver), MCF-7 (breast), and HeLa (cervical). Both the in vitro cytotoxicity of acridinedione derivatives (1a-1j) on normal cells (Table 3) and the results of the cytotoxic screening of compounds (1a-1j) are shown in Table 2.

3.5. Molecular Docking interaction results

To better grasp the future development of biological response, docking studies were added as docking studies can provide an understanding on biological activities of the molecule [38–43]. Docking effects of compounds **1a-1j** and Doxorubicin regulation with protein 1Z11 were evaluated using the Autodock Vina programme [38–39]. The binding affinity of compound 1h for the 1Z11 protein is greater than that

Scheme 2. Plausible mechanism for the formation of the catalyzed by AgNPs.

of any other compound (-11.7 kcal/mol), whereas the binding affinity of Doxorubicin is lower (-10.2) kcal/mol. Compound 1h establishes a single hydrogen bond with the 1Z11 receptor. The hydrogen bonding interaction included the amino acid residue Arg101 (bond length: 5.85). Val117, Gly301, Gly302, Thr305, Ile366, Leu370, Cys433, and Ala445 were all involved in hydrophobic interactions via the formation of three hydrogen bonds with the 1Z11 receptor, doxorubicin controls it. The hydrogen bonding interaction included the amino acid residues Leu370

Michael adduct

(2.38, 2.61) and Phe440 (2.97). Hydrophobic interactions were shown to be of relevance to Val117, Leu298, Ser369, Cys439, and Gly441. Figs. 7-8 show the hydrogen bonding and hydrophobic interactions of amino acid residues in the 1Z11 protein with the 1a-1j and Doxorubicin compounds, respectively. The results indicate that the target protein's compound 1h has a significant inhibitory effect on Doxorubicin. Interaction data from Molecular Docking is shown in Tables 4 and 5 [40–43].

Table 4
Molecular docking interaction of compounds 1a-1j and Doxorubicin against protein 1Z11.

Compound	Human microsomal cytochrome P450 2A6 complexed with methoxsalen (PDB ID: 1Z11)				
	Binding affinity (kcal/mol)	No. of H- bonds	H-bonding residues		
1a	-10.6	-	-		
1b	-8.3	2	Arg128 and Gly301		
1c	-6.8	1	Leu370		
1d	-8.1	4	Val116, Val117, Gly301 and Arg437		
1e	-8.0	2	Thr309 and Gln360		
1f	-7.8	1	Thr309		
1g	-8.2	2	Thr309 and Gln360		
1h	-11.7	1	Arg101		
1i	-5.3	0	-		
1j	-11.0	1	Leu370		
Doxorubicin	-10.2	3	Leu370 and Phe440		

4. Conclusion

Finally, we concentrate on a green and safe method for producing silver nanoparticles (AgNPs) using Vitex negundo extract, which can easily convert silver ions into AgNPs. In the synthesis of acridinedione analogues in aqueous ethanol, these nanoparticles demonstrate exceptional catalytic ability employing a one-pot three-component condensation of 1,3-cyclohexanedione variations, aniline with substituted aldehyde, and AgNPs as a green catalyst. The cytotoxicity of the acridinedione compounds was assessed using the MTT test with doxorubicin as the reference drug against three cancer cell lines and three normal cell lines (human embryonic kidney cell (HEK293), liver cell (LO2), and lung cell (MRC5). When compared to other compounds examined for the same purpose (HepG2, LC50-0.5 M, MCF-7, LC50-0.64 M, and HeLa, LC₅₀-0.52), compound 1h shown substantial activity. The IC₅₀ values for cytotoxicity in normal cell lines (HEK-293, LO2, and MRC5) were all greater than 100 g/mL, showing the compounds' safety. In comparison to other medications, **1h** has a higher binding affinity (-11.7 kcal/mol) for the 1Z11 protein, whereas Doxorubicin has a lower affinity (-10.2 kcal/mol). As a result, compound 1h holds significant potential as a molecule for use in the development of cancer therapeutics.

Table 5Hydrophobic interaction of synthesized compounds (1a-1j) and Doxorubicin

Compounds	Hydrophobic interaction								
	Vander Waals	Conventional H- Bond	Pi-sigma	Pi-Sulfur	Pi-Pi T shaped	Alkyl	Pi-alkyl		
1a	Arg369								
	Ser433 Arg437	-	Leu370	Cys439	-	Ile366	Val365		
	Asn438 Phe480		Dhr305						
1b	Phe209								
	Phe480	Gly301	Thr305	-	Phe118	Cos439	Ile336		
	Phe111	Arg128			Phe107	Val117	Leu370		
	Asn297								
	Leu298								
1c	Phe440								
	Gly301	Leu370	-	-	Phe432	Val365	Pro431		
	Phe118						Cos439		
	Phe209								
	Ser369								
1d	Phe209	Val116							
	Phe480	Val117	Thr305	-	Phe118	Ile336	Ile300		
	Phe111	Arg437			Phe107	Leu376	Cys439		
	Leu298	Gly301							
_	Phe440								
1e	Phe118	01.000			m1 440	** 10.5			
	Ile300	Gln360	Gly301	Cys439	Phe440	Val365	Leu298		
	Ser369	Thr309			Asn297	Leu370	Val117		
	Thr305								
	Val306					** 10.5			
1f	Phe209	mi 000	61.001		Pl 400	Val365			
	Ile300	Thr309	Gly301	-	Phe480	Cys439	Leu370		
	Arg101				Asn297	Leu298			
	Phr305					Val117			
	Pro431			0 400	Pl 400	V 1065	** 11.17		
1g	Asn297	G1 000		Cys439	Phe480	Val365	Val117		
	Ile300	Gln360	-		Phe440		Leu370		
	Phe209	Thr309							
	Ser369								
11.	Phr307	A==101		C===420		11-266	A10.44E I 04.27		
1h 1i	Gly302	Arg101	-	Cys439	-	Ile366	Ala445 Leu37		
11	Gly302 Ile300		Db a 422	C+++420	Db a 440	I au 270	11-266		
	Phe209	-	Phe432	Cys439	Phe440	Leu370	Ile366		
	Ala445								
	Thr305								
1j	Phe480								
±J	Leu298	Leu370	_	Cys439	Phe440	Val117	Ile366		
	Gly441	Ecu3/ U	-	Сузтоэ	1 HCTTU	V 011 1 /	116300		
	Val306								
	Thr305								
Dox	-	Leu370	_	Cys439	_	_	_		
DUA		Phe440	-	Gyoros		-	-		

CRediT authorship contribution statement

Perumal Gobinath: Writing – original draft, Visualization, Validation, Investigation, Formal analysis, Conceptualization. Ponnusamy Packialakshmi: Visualization, Validation, Investigation, Formal analysis. Govindasamy Thilagavathi: Writing – original draft, Investigation, Formal analysis, Data curation. Natarajan Elangovan: Writing – original draft, Visualization, Validation, Resources, Methodology, Investigation, Formal analysis, Data curation, Conceptualization. Renjith Thomas: Writing – original draft, Visualization, Validation, Supervision, Software, Resources, Formal analysis, Data curation. Radhakrishnan Surendrakumar: Writing – original draft, Visualization, Validation, Supervision.

Declaration of competing interest

The authors declare that they have no known competing financial interests or personal relationships that could have appeared to influence the work reported in this paper.

Data availability

Data will be made available on request.

Acknowledgments

We wish to thank Government of India for providing DST-FIST (SR/FST/COLLEGE-372/2018) fund for Nehru Memorial College, Puthanampatti, Trichy, Tamil Nadu, India.

Funding

No funds were received.

Supplementary materials

Supplementary material associated with this article can be found, in the online version, at doi:10.1016/j.chphi.2024.100483.

References

- J.M. Reichert, JB. Wenger, Development trends for new cancer therapeutics and vaccines, Drug Discov. Today 13 (2008) 30–37.
- [2] I. Ali, M.N. Lone, H.Y. Aboul-Enein, Imidazoles as potential anticancer agents, medChemComm 8 (2017) 1742–1773.
- [3] American Cancer Society, Cancer Facts & Figures, The Society, 2008.
- [4] J.R. Molina, P. Yang, S.D. Cassivi, S.E. Schild, AA. Adjei, Non-small cell lung cancer: epidemiology, risk factors, treatment, and survivorship, Mayo Clin. Proc. 83 (2008) 584–594. Elsevier.
- [5] S. Navada, P. Lai, A.G. Schwartz, GP. Kalemkerian, Temporal trends in small cell lung cancer: analysis of the national Surveillance, Epidemiology, and End-Results (SEER) database, J. Clin. Oncol. 24 (2006) 7082.
- [6] T. Sher, G.K. Dy, AA. Adjei, Small cell lung cancer, Mayo Clin. Proc. 83 (2008) 355–367, https://doi.org/10.1016/j.ijrobp.2017.06.2452. Elsevier.
- [7] C.S. Grasso, Y.M. Wu, D.R. Robinson, X. Cao, S.M. Dhanasekaran, A.P. Khan, S. A. Tomlins, The mutational landscape of lethal castration-resistant prostate cancer, Nature 487 (2012) 239–243, https://doi.org/10.1038/nature11125.
- [8] G.A. Elmegeed, H.H. Ahmed, JS. Hussein, Novel synthesized aminosteroidal heterocycles intervention for inhibiting iron-induced oxidative stress, Eur. J. Med. Chem. 40 (2005) 1283–1294, https://doi.org/10.1016/j.eimech.2005.07.012.
- [9] N. Vigneshwaran, N.M. Ashtaputre, P.V. Varadarajan, R.P. Nachane, K. M. Paralikar, R.H. Balasubramanya, Biological synthesis of silver nanoparticles using the fungus Aspergillusflavus, Mater. Lett. 61 (2007) 1413–1418, https://doi.org/10.1016/j.matlet.2006.07.042.
- [10] P. Mohanpuria, N.K. Rana, SK. Yadav, Biosynthesis of nanoparticles: technological concepts and future applications, J. Nanoparticle Res. 10 (2008) 507–517, https://doi.org/10.1007/s11051-007-9275-x
- [11] S.S. Shankar, A. Rai, A. Ahmad, M. Sastry, Rapid synthesis of Au, Ag, and bimetallic Au core–Ag shell nanoparticles using Neem (Azadirachta indica) leaf broth, J. Colloid. Interface Sci. 275 (2004) 496–502, https://doi.org/10.1016/j. jcis.2004.03.003.

- [12] I. Willner, R. Baron, B. Willner, Growing metal nanoparticles by enzymes, Adv. Mater. 18 (2006) 1109–1120, https://doi.org/10.1002/adma.200501865.
- [13] V.C. Verma, R.N. Kharwar, AC. Gange, Biosynthesis of antimicrobial silver nanoparticles by the endophytic fungus Aspergillus clavatus, Nanomedicine 5 (2010) 33–40, https://doi.org/10.2217/nnm.09.77.
- [14] S. Gurunathan, J.H. Park, J.W. Han, JH. Kim, Comparative assessment of the apoptotic potential of silver nanoparticles synthesized by Bacillus tequilensis and Calocybe indica in MDA-MB-231 human breast cancer cells: targeting p53 for anticancer therapy, Int. J. Nanomed. 10 (2015) 4203–4223, https://doi.org/ 10.2147/IJN.883953.
- [15] W.R. Li, X.B. Xie, Q.S. Shi, H.Y. Zeng, Y.S. Ou-Yang, YB. Chen, Antibacterial activity and mechanism of silver nanoparticles on Escherichia coli, Appl. Microbiol. Biotechnol. 85 (2010) 1115–1122, https://doi.org/10.1007/s00253-009-2159-5.
- [16] P. Mukherjee, A. Ahmad, D. Mandal, S. Senapati, S.R. Sainkar, M.I. Khan, M. Sastry, Fungus-mediated synthesis of silver nanoparticles and their immobilization in the mycelial matrix: a novel biological approach to nanoparticle synthesis, Nano Lett. 1 (2001) 515–519, https://doi.org/10.1021/nl0155274.
- [17] S. Chernousova, M. Epple, Silver as antibacterial agent: ion, nanoparticle, and metal, Angew. Chem. Int. Ed. 52 (2013) 1636–1653, https://doi.org/10.1002/ ania 201205023
- [18] J. Joseph, E. Kuruvilla, A.T. Achuthan, D. Ramaiah, GB. Schuster, Tuning of intercalation and electron-transfer processes between DNA and acridinium derivatives through stericeffects, Bioconjugatechemistry 15 (2004) 1230–1235, https://doi.org/10.1021/bc0498222.
- [19] P. Belmont, I. Dorange, Acridine/acridone: a simple scaffold with a wide range of application in oncology, Expert. Opin. Ther. Pat. 18 (2008) 1211–1224, https:// doi.org/10.1517/13543776.18.11.1211.
- [20] A. Souibgui, A. Gaucher, J. Marrot, F. Bourdreux, F. Aloui, B.B. Hassine, D. Prim, New series of acridines and phenanthrolines: synthesis and characterization, Tetrahedron 70 (2014) 3042–3048, https://doi.org/10.1016/j.tet.2014.02.067.
- [21] M. Kozurkova, S. Hamulakova, Z. Gazova, H. Paulikova, P. Kristian, Neuroactive multifunctional tacrine congeners with cholinesterase, anti-amyloid aggregation and neuroprotectiveproperties, Pharmaceuticals 4 (2011) 382–418, https://doi. org/10.3390/ph4020382.
- [22] A. Srivastava, A. Nizamuddin, Synthesis and fungicidal activity of some acridine derivatives. Indian J. Heterocyclic Chem. 13 (2011) 261–264.
- [23] Y. Mikata, M. Yokoyama, K. Mogami, M. Kato, I. Okura, M. Chikira, S. Yano, Intercalator-linked cisplatin: synthesis and antitumor activity of cisdichloroplatinum (II) complexes connected to acridine and phenylquinolines by one methylene chain, Inorganicachimica Acta 279 (1998) 51–57, https://doi.org/ 10.1016/S0020-1693(98)00035-8.
- [24] S.A. Gamage, J.A. Spicer, G.J. Atwell, G.J. Finlay, B.C. Baguley, W.A. Denny, Structure activity relationships for substituted bis (acridine-4-carboxamides): a new class of anticancer agents, J. Med. Chem. 42 (1999) 2383–2393, https://doi.org/10.1021/jm980687. https://doi.org/10.1007/s00044-012-0236-2c). 10.1080/00397910802044306. mb da Rocha Pitta M G, Souza ÉS, Barros FWA, Moraes Filho MO, Pessoa CO, Hernandes MZ, da Rocha Pitta I. Synthesis and in vitro anticancer activity of novel thiazacridine derivatives. Medicinal Chemistry Research, 2013;22:2421-2429. Venkatesan, K, Pujari, S.S & Srinivasan, K.V. Proline-catalyzed simple and efficient synthesis of1,8-dioxo-decahydroacridines in aqueous ethanol medium. SyntheticCommunications, 2008;39:228241.
- [25] (a) M. Kaya, E. Basar, E. Çakir, E. Tunca, M. Bülbül, Synthesis and characterization of novel dioxoacridinesulfonamide derivatives as new carbonic anhydrase inhibitors, J. Enzyme Inhib. Med. Chem. 27 (2012) 509–514, https://doi.org/10.3109/14756366.2011.599029;
 (b) U.R. Yeşildaği, E. Başar, M. Aslan, M. Kaya, M. Bülbül, Facile, highly efficient, and clean one-pot synthesis of acridine sulfonamide derivatives at room temperature and their inhibition of human carbonic anhydrase isoenzymes, Monatshefte für Chemie–Chem. Month. 145 (2014) 1027–1034, https://doi.org/10.1007/s00706-013-1145-x
- [26] (a) B. Das, P. Thirupathi, I. Mahender, V.S. Reddy, YK. Rao, Amberlyst-15: an efficient reusable heterogeneous catalyst for the synthesis of 1, 8-dioxo-octahy-droxanthenes and 1,8-dioxo-decahydroacridines, J. Mol. Catal. A: Chem. 247 (2006) 233–239, https://doi.org/10.1016/j.molcata.2005.11.048;
 (b) M. Kaya, Y. Yıldırır, GY. Çelik, Synthesis and antimicrobial activities of novel bisacridine-1,8-dione derivatives, Med. Chem. Res. 20 (2011) 293–299, https://doi.org/10.1007/s00044-010-9321-6.
- [27] G.M. Ziarani, A. Badiei, M. Hassanzadeh, S. Mousavi, Synthesis of 1,8-dioxo-dec-ahydroacridine derivatives using sulfonic acid functionalized silica (SiO2-Pr-SO3H) under solvent free conditions, Arab. J. Chem. 7 (2014) 335–339, https://doi.org/10.1016/j.arabjc.2011.01.037.
- [28] J. George, J.C. Prasana, S. Muthu, T.K. Kuruvilla, S. Sevanthi, R.S. Saji, Spectroscopic (FT-IR, FT Raman) and quantum mechanical study on N-(2, 6dimethylphenyl)-2-{4-(12-hydroxy-3-(2-methoxyphenoxy) propyl] piperazin-1-yl} acetamide, J. Mol. Struct. 1171 (2018) 268–278, https://doi.org/10.1016/j. molstruc.2018.05.106.
- [29] S. Muthu, G. Ramachandran, Spectroscopic studies (FTIR, FT-Raman and UV-Visible), normal coordinate analysis, NBO analysis, first order hyper polarizability, HOMO and LUMO analysis of (1R)-N-(Prop-2-yn-1-yl)-2, 3-dihydro-1H-inden-1-amine molecule by a binitio HF and density functional methods, Spectrochim. Acta Part A: Mol. Biomol. Spectrosc. 121 (2014) 394–403, https://doi.org/10.1016/j.saa.2013.10.093.
- [30] G. Bharathy, J.C. Prasana, S. Muthu, A. Irfan, F.B. Asif, A. Saral, S. Aayisha, Evaluation of electronic and biological interactions between N-[4-(Ethylsulfamoyl) phenyl] acetamide and some polar liquids (IEFPCM solvation model) with Fukui

- function and molecular docking analysis, J. Mol. Liq. 340 (2021) 117271, https://doi.org/10.1016/j.molliq.2021.117271.
- [31] S. Sevvanthi, S. Muthu, M. Raja, S. Aayisha, S. Janani, PES, molecular structure, spectroscopic (FT-IR, FT-Raman), electronic (UV-Vis, HOMO-LUMO), quantum chemical and biological (docking) studies on a potent membrane permeable inhibitor: dibenzoxepine derivative, Heliyon 6 (8) (2020), https://doi.org/10.1016/j.heliyon.2020.e04724.
- [32] A. Thamarai, R. Vadamalar, M. Raja, S. Muthu, B. Narayana, P. Ramesh, S. Aayisha, Molecular structure interpretation, spectroscopic (FT-IR, FT-Raman), electronic solvation (UV-Vis, HOMO-LUMO and NLO) properties and biological evaluation of (2E)-3-(biphenyl-4-yl)-1-(4-bromophenyl) prop-2-en-1-one: experimental and computational modeling approach, Spectrochim. Acta Part A: Mol. Biomol. Spectrosc. 226 (2020) 117609, https://doi.org/10.1016/j. saa.2019.117609.
- [33] N.J. Marshall, C.J. Goodwin, S.J Holt, A critical assessment of the use of microculture tetrazolium assays to measure cell growth and function, Growth Regul. 5 (1995) 69–84.
- [34] O. Trott, AJ. Olson, AutoDock Vina: improving the speed and accuracy of docking with a new scoring function, efficient optimization, and multithreading, J. Comput. Chem. 31 (2010) 455–461, https://doi.org/10.1002/jcc.21334.
- [35] F.C. Bernstein, T.F. Koetzle, G.J. Williams, E.F. Meyer Jr, M.D. Brice, J.R. Rodgers, M. Tasumi, The Protein Data Bank: a computer-based archival file for macromolecular structures, J. Mol. Biol. 112 (1977) 535–542, https://doi.org/10.1016/S0022-2836/7780200-3
- [36] J.K. Yano, M.H. Hsu, K.J. Griffin, C.D. Stout, EF. Johnson, Structures of human microsomal cytochrome P450 2A6 complexed with coumarin and methoxsalen, Nat. Struct. Mol. Biol. 12 (2005) 822–823, https://doi.org/10.1038/nsmb971.

- [37] M.R. Boyd, KD. Paull, Some practical considerations and applications of the National Cancer Institute in vitro anticancer drug discovery screen, Drug Dev. Res. 34 (1995) 91–109, https://doi.org/10.1002/ddr.430340203.
- [38] G.M. Morris, R. Huey, W. Lindstrom, M.F. Sanner, R.K. Belew, D.S. Goodsell, A. J. Olson, AutoDock4 and AutoDockTools4: automated docking with selective receptor fleshility, J. Comput. Chem. 30 (2009) 2785–2791, https://doi.org/10.1002/jcs.21256
- [39] Discovery Studio BIOVA, Discovery Studio Client V17, San Diego, Dassault Systems, 2017. http://accelrys.com/products/collaborative-science/biovia-discovery-studio/.
- [40] J.A. Agwupuye, H. Louis, T.O. Unimuke, P. David, E.I. Ubana, Y.L. Moshood, Electronic structure investigation of the stability, reactivity, NBO analysis, thermodynamics, and the nature of the interactions in methyl-substituted imidazolium-based ionic liquids, J. Mol. Liq. 337 (2021) 116458, https://doi.org/ 10.1016/j.molliq.2021.116458.
- [41] E.A. Eno, J.I. Mbonu, H. Louis, F.S. Patrick-Inezi, T.E. Gber, T.O. Unimuke, E.E. D. Okon, I. Benjamin, O.E. Offiong, Antimicrobial activities of 1-phenyl-3-methyl-4-trichloroacetyl-pyrazolone: experimental, DFT studies, and molecular docking investigation, J. Indian Chem. Soc. 99 (2022) 100524.
- [42] H. Louis, T.E. Gber, F.C. Asogwa, E.A. Eno, T.O. Unimuke, V.M. Bassey, B.I. Ita, Understanding the lithiation mechanisms of pyrenetetrone-based carbonyl compound as cathode material for lithium-ion battery: insight from first principle density functional theory, Mater. Chem. Phys. 278 (2022) 125518, https://doi.org/ 10.1016/j.matchemphys.2021.125518.
- [43] P. Nkoe, A.L.E. Manicum, H. Louis, F.P. Malan, W.J. Nzondomyo, K. Chukwuemeka, S.A. Sithole, A. Imojara, C.M. Chima, E.C. Agwamba, T. O. Unimuke, Influence of solvation on the spectral, molecular structure, and antileukemic activity of 1-benzyl-3-hydroxy-2-methylpyridin-4(1H)-one, J. Mol. Liq. 370 (2023) 121045, https://doi.org/10.1016/j.molliq.2022.121045.